====== **SEMICONDUCTORS** ======

Dielectric and Electrical Properties of Polymorphic Bismuth Pyrostannate $Bi_2Sn_2O_7$

L. V. Udod[a, b, *], **S. S. Aplesnin**[a, b], **M. N. Sitnikov**[a], **and M. S. Molokeev**[b]

[a] *Reshetnev Siberian State Aerospace University,*
pr. imeni Gazety "Krasnoyarskii Rabochii" 31, Krasnoyarsk, 660014 Russia
* e-mail: luba@iph.krasn.ru
[b] *Kirensky Institute of Physics, Siberian Branch of the Russian Academy of Sciences,*
Akademgorodok 50–38, Krasnoyarsk, 660036 Russia
Received January 16, 2014

Abstract—The $Bi_2Sn_2O_7$ compound existing simultaneously in two polymorphic modifications, namely, orthorhombic and cubic, has been synthesized for the first time by solid-phase synthesis. The dielectric and electrical properties of the compound have been studied in the temperature range $100\ K < T < 500\ K$. Anomalies in the temperature dependences of the electrical resistivity and the permittivity (imaginary and real parts) have been found at both low and high temperatures. These features are explained in terms of the model of martensitic phase transitions.

1. INTRODUCTION

At present, the study and search for sensors operating on the basis of physical principles are important problems. The principle of the operation of semiconductor gas sensors is based on the dependence of the electrical conductivity of a sensitive sensor layer on the gas concentration in the environment. The effect of varying the conductivity of semiconductors upon absorption of various molecules from a gaseous phase on their surfaces is successively used to detect gases by semiconductor sensors with an electron conductivity based on SnO_2, TiO_2, WO_3, V_2O_5, In_2O_3, Fe_2O_3, Cu_2O, CuO, ZnO, CdO, NiO, and others [1–3]. Oxide semiconductor detectors determine the gas concentration by measuring the electrical resistivity of a sensor device element contacting with gas under determination.

Extensive studies of semiconductor oxide gas sensors for recent 15–20 years collected great theoretical and experimental data arrays. In this connection, further progress in this field of science and engineering needs expansion of a class of materials exhibiting sensor properties and searching for new ways to solving the problem of metal oxide-based chemical sensors. Among such materials are not only simple metal oxides mainly exhibiting variable valence but also their compounds, e.g., $CaZrO_3$, $SrCeO_3$, $BiFeO_3$, $Bi_2Sn_2O_7$, $BaTiO_3$, and $BaTi_{1-x}Sn_xO_3$. In particular, bismuth pyrostanate $Bi_2Sn_2O_7$ is used in gas sensors as a detector for determining carbon monoxide in the presence of other gases.

Bismuth pyrostannate has important practical application; however, the available data on its properties, in particular, stability, phase and polymorphic transformations are very contradictory. According to [4, 5], there are three crystallographic phases: the tetragonal α-$Bi_2Sn_2O_7$ ($a = 21.328$ Å, $c = 21.545$ Å) existing to 90°C; the cubic β-$Bi_2Sn_2O_7$ ($a = 21.4$ Å) existing between 90 and 680°C; the cubic face-centered γ-$Bi_2Sn_2O_7$ ($a = 10.73$ Å) existing above 680°C. According to the Raman spectroscopy data [6], the temperature dependence of the phonon mode intensity demonstrates a structural $\alpha \longrightarrow \beta$ transition about 127°C. The IR spectrum of $Bi_2Sn_2O_7$ [7] differs significantly from typical spectra of stannates with a cubic pyrochlore-like structure.

The theoretical calculations of the electronic structure by the electron density functional method [8] for stannates with the cubic lattice revealed a gap of ~2 eV in the spectrum of electronic excitations; i.e. stannates are semiconductors and must have a semiconductor type of conduction. Neither transport properties nor dielectric properties of $Bi_2Sn_2O_7$ were studied even at low temperatures. The changes occurring in the crystal lattice or softening of phonon vibration modes can be found from the temperature dependences of the permittivity.

A complex nature of bismuth oxide-based systems leads to ambiguous information on polymorphic transitions, temperatures and origin of phase transformations.

The aim of this work is to synthesize a $Bi_2Sn_2O_7$ compound and to study its electrical and dielectric
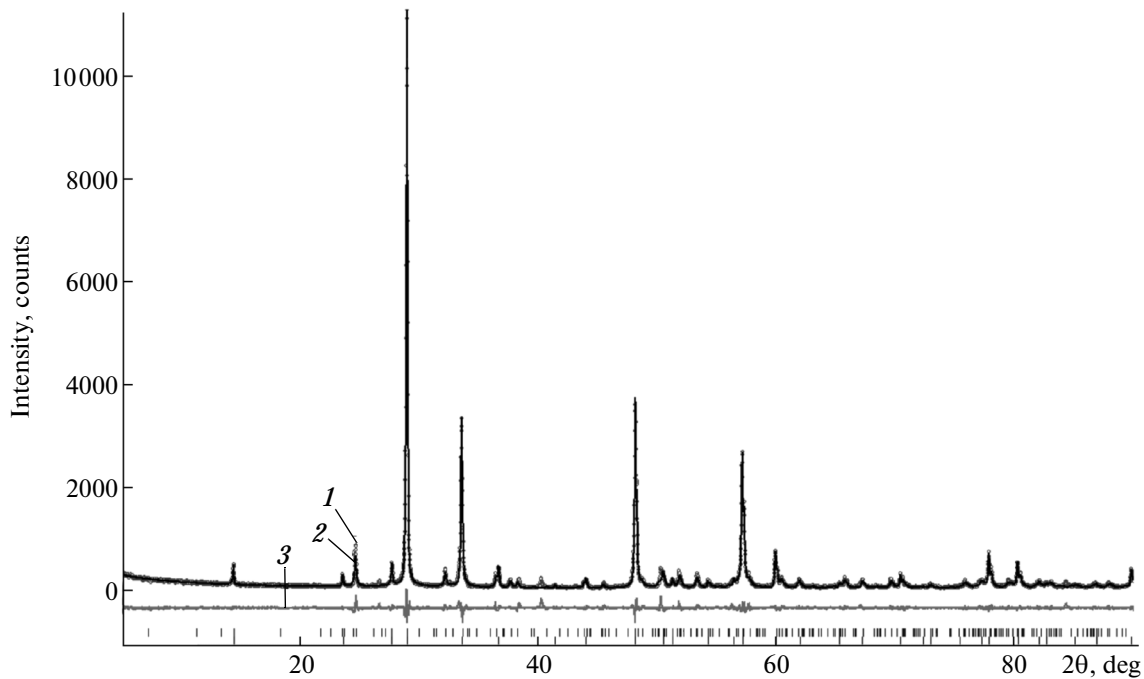
Fig. 1. Differential X-ray diffraction pattern of $Bi_2Sn_2O_7$: (*1*) experimental diffraction pattern, (*2*) theoretical diffraction pattern, (*3*) difference between the theoretical and experimental diffraction patterns.

2. SAMPLE SYNTHESIS AND EXPERIMENTAL RESULTS

Experimental studies of phase equilibria in bismuth oxide-based systems are hampered because of chemical aggression of liquid bismuth oxide with respect to crucible materials and are complicated by the formation of metastable phases. Because of this, to synthesize $Bi_2Sn_2O_7$, we chose the solid-phase reaction method with multiple careful and prolonged intermediate grindings in alcohol. As initial materials, high-pure oxides Bi_2O_3 and SnO_2 were used. An initial oxide mixture pressed into pellets was placed in a furnace and held at temperatures from 700 to 950°C; the holding time was varied from 8 to 24 h.

The X-ray diffraction studies of the synthesized samples were performed on a Bruker D8 ADVANCE diffractometer (CuK_α-radiation; a VANTEC detector) at room temperature (Fig. 1). The results show that the sample consists of two polymorphic modifications of $Bi_2Sn_2O_7$ (cubic ($Fd-3m$, $a = 10.6924(2)$ Å, $V = 1222.42(9)$ Å^3) and orthorhombic ($Pmmm$, $a = 3.7825(2)$ Å, $b = 7.9083(6)$ Å, $c = 12.3276(8)$ Å, $V = 368.71(4)$ Å^3)) existing simultaneously. Judging from the ratio of reflection intensities, the percentage of the cubic phase is higher than that of the orthorhombic phase. It is impossible to precisely determine the percent ratio of the phases because of the absence of the

orthorhombic phase structure. The structure can be found only from an X-ray diffraction pattern of a pure-phase sample. A comparison of the unit cell parameters of the orthorhombic phase with known $Bi_2Sn_2O_7$ phases [4, 9–12] shows that new phase has no analogs. The difference in the crystal structures is due to different technologies of obtaining the compound. In polycrystalline samples, grains form and grow with decreasing temperature; in this case, the grain size is dependent on the annealing time. At the same time, the grain size is dependent on the time and carefulness of grinding. A long time and carefulness of grinding in ethanol are sufficient conditions of the formation of a two-phase $Bi_2Sn_2O_7$ sample.

The permittivity of $B_2Sn_2O_7$ was measured on an LCR-829 METER setup in the temperature range 100–500 K at a frequency of 100 kHz. An analysis of the experimental data shows an increase in the permittivity with increasing temperature. The temperature dependence of the real part of the permittivity Re(ε) depicted in Fig. 2 has a maximum in the vicinity of a temperature of 450 K, and the slope of Re(ε) (*T*) is changed at 200 K. The temperature dependence of the imaginary part of the permittivity Im(ε) (Fig. 3) has several kinks and clear maxima at temperatures about 200, 340, and 450 K.

The electrical properties of $Bi_2Sn_2O_7$ were measured by the four-probe method on an Aglient Technologies Multimeter 344 10A device in the temperature range 200–600 K. Figure 4 shows the temperature dependence of the resistivity which can be conven-
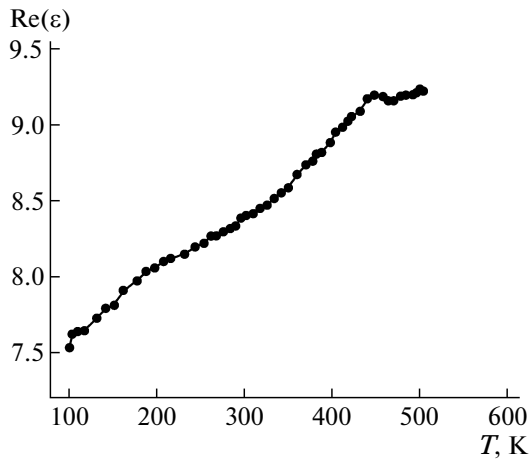
Fig. 2. Temperature dependence of the real part of the permittivity of $Bi_2Sn_2O_7$ at a frequency $\omega = 100$ kHz.

Fig. 3. (a) Temperature dependence of the imaginary part of the permittivity of $Bi_2Sn_2O_7$ at a frequency $\omega = 100$ kHz; and (b) temperature dependence of the inverse optical conductivity of $Bi_2Sn_2O_7$ at a frequency $\omega = 100$ kHz.

tionally separated into three segments. The first segment is the decrease in the resistivity from $\rho \sim 10^8$ to $\sim 10^6$ Ω cm in the temperature range 200–330 K; in this segment, sharp anomalies are observed at 245–290 K. Then, the resistivity increases by an order of magnitude in the range from 330 to 450 K, and, then, decreases within the order of ρ. In the temperature range 330–600 K, a wide maximum is observed about 450 K.

Activation energy $\Delta E_1 = 0.23$ eV was calculated from temperature dependence $\log(\rho/10^3 T)$ described by linear function $\ln \rho = \ln \rho_{01} + (\Delta E_1/k_B T)$, where k_B is the Boltzmann constant. The decrease in the activation energy as compared to the theoretical data [8] is due to the impurity type of conduction.

3. DISCUSSIONS OF THE RESULTS

The imaginary part of the permittivity can be used to determine optical conductivity $\sigma = \varepsilon_0 Im(\varepsilon)\omega$ and resistivity $\rho = 1/\sigma$ whose temperature dependence (Fig. 3) is qualitatively different from that of the dc resistivity. The reason of the difference can be a polarization current due to vibrations of a nonuniform electrical charge on domains between two phases or defects on cations or anions. In both cases, the vibration amplitudes increase, e.g., with both a decrease in the density of domain interphase boundaries with increasing temperature and an increase in the fraction of the bulk cubic phase whose unit cell volume is significantly larger than the unit cell volume in the orthorhombic phase. The permittivity also has a maximum in the structural transition region.

When temperature decreases, the two-phase state detected at room temperature transforms into the single-phase orthorhombic state at $T = 200$ K. Similar phenomena were observed in manganites doped with rare-earth elements which contained two crystallo-

graphic ($P2_1/m$ and $Pnma$) and two antiferromagnetic phases [13–15]. The proportion between the phases can be varied by magnetic field; e.g., the neutron diffraction experiment on $Ca_{0.85}Sm_{0.15}MnO_3$ [6] revealed an increase in the orthorhombic phase volume to 56% in magnetic field of 60 kOe at $T = 100$ K due to the decrease in the monoclinic phase volume from 94 to 44%. The existence of two phases of these compounds is a result of doping $CaMnO_3$ with various rare-earth ions, which leads to the change in the structure and magnetic properties [17, 18].
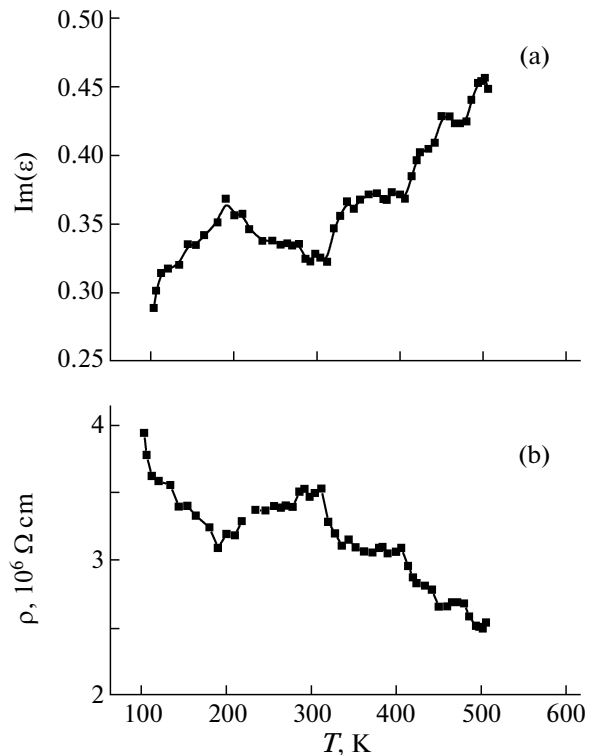
In our case, the sample already exists in the two-phase state because of the preparation technology. The coexistence of two crystallographic structures is observed in the temperature range 200–450 K; as temperature increases, the compound transforms into the state with the cubic structure at $T = 450$ K. These polymorphic transitions can be considered as martensitic transitions. A martensitic transformation is a transformation of a crystal lattice without diffusion; it is characteristic of steels, metals, semiconductors, and polymers which manifest polymorphism. This phenomenon is most studied in iron carbon alloys; at high temperatures in the austenite state, the alloy has a cubic lattice (γ-phase); during cooling, the alloy transforms into a martensitic phase (α-phase) in which the lattice unit cells become canted parallelepipeds [19].

ρ, Ω cm
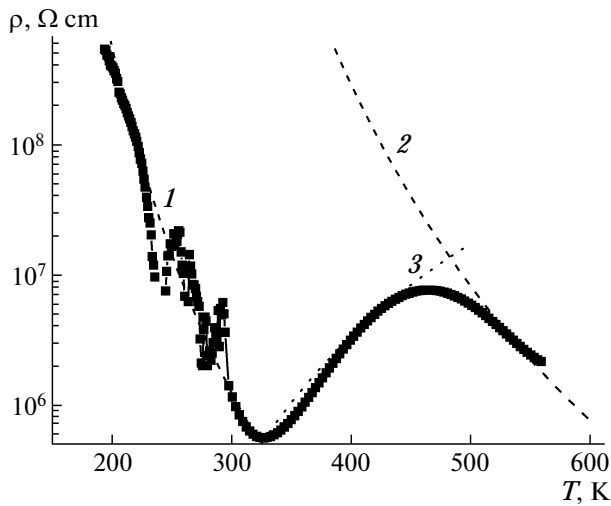
Fig. 4. Temperature dependence of the resistivity of $Bi_2Sn_2O_7$. The experimental curve is shown by black squares, and the dashed lines show the theoretical calculation: (*1*) $\rho = \rho_{01}\exp(\Delta E_1/k_B T)$, (*2*) $\rho = \rho_{02}\exp(\Delta E_2/k_B T)$, (*3*) $\rho = \rho_0\exp(\Delta E/k_B T)$ with $\rho = 5 \times 10^5$, $\Delta E = 0.28$ eV, $\rho_{01} = 6.2$ Ω cm, $\Delta E_1 = 0.23$ eV, $\rho_{02} = 5.2$ Ω cm, $\Delta E_2 = 0.51$ eV.

Manganites also undergo martensitic transitions [13, 20] accompanied by maxima in the temperature dependence of the resistivity.

To study the effect of temperature on the existence of the polymorphic transitions in $Bi_2Sn_2O_7$, we chose a technique of measuring the temperature dependence of the resistivity. The technique demonstratively reflects phase transformations occurring in the material. As is seen from Fig. 4, with increasing temperature, the resistivity deviates from the exponential dependence with low jumps in the temperature range 200–330 K. Similar behavior of the resistivity was observed in Heusler alloys Ni_2MnX (X = Ga, Sn, In, Co) [21, 22]. This behavior is associated with the fact that the austenite (cubic) phase has a higher symmetry as compared to the martensite (orthorhombic) phase and a lower resistivity. It seems likely that, in the temperature range 200–450 K, $Bi_2Sn_2O_7$ undergoes the martensitic transition from the orthorhombic to cubic phase. The existence of sharp anomalies in this range indicates that the structure contains domains in the form of grains with various orientations in the sample. As temperature decreases, the domain boundaries increase and the difference in their orientations increases. A change in the domain density causes anomalies of the resistivity. Such scheme is characteristic of martensitic transitions in metals and semiconductors. It is noted that a martensitic transition in polycrystalline samples is very sensitive to the grain size which depends on the synthesis technology. Polycrystalline $La_{0.275}Pr_{0.35}Ca_{0.375}MnO_3$ [20] has a cubic crystal lattice at $T = 300$ K; at $T \approx 210$ K, lens-shaped

and lamellar domains nucleate and grow in each of the grains. Further cooling increases the differences in the domain forms, which is a result of structural deformations. In [20], the dependence of the transport properties on the grain size was found from the temperature dependence of the resistivity. With decreasing grain size, the maximum in curve $\rho(T)$ shifts toward lower temperatures., and the resistivity increases from 0.1 to 10^8 Ω cm. A change in the grain size is a reason of the transition of the compound from the metallic state to the insulator state, and the samples with the smallest grain size do not undergo any metal–insulator transition.

In this work, the activation energy of bismuth stannates in the cubic phase is $\Delta E_2 = 0.51$ eV at $T > 450$ K and increases by a factor of 1.8 as compared to that of the orthorhombic structure. The increase in the resistivity in the temperature range 320 K $< T <$ 450 K can be explained in the model of coexistence of two phases, when the percolation over the orthorhombic phase disappears, and the cubic phase contains islands of the martensite (low-temperature) phase. The region of the islands decreases with increasing temperature, and the width of the potential barrier formed by the cubic high-resistivity phase increases. This can be represented as a model of potential wells, in which linear sizes and number of electrons in a well decrease. The potential barrier increases with increasing temperature and, it is possible, will change according to a linear law $\Delta E = (\Delta E_2 - \Delta E_1)(T/T^* - 1)$. The charge carrier mobility relating to hopping electrons over the islands will be determined by electron tunneling $\mu \sim \exp(-\Delta E/kT)$. The resistivity will increase with increasing temperature to $T = 450$ K, as shown in Fig. 4 by the dashed line, when the carrier mobility in the matrix becomes equal to the tunneling electron mobility.

Figure 4 shows the result of calculation of the resistivity with fitting parameters $\rho = \rho_0\exp(\Delta E/k_B T)$ with $\rho_0 = 5 \times 10^5$, $\Delta E = 3280$ K, $T^* = 325$ K. The model adequately explains the experimental data and agrees with the structural studies [4, 9–12], according to which bismuth stannates $Bi_2Sn_2O_7$ is in the single-phase state with the cubic β-phase at high temperatures.

4. CONCLUSIONS

We developed the technology of synthesizing the $Bi_2Sn_2O_7$ compound with a new crystal lattice. It is found that, at room temperature, the compound has the two-phase state with the orthorhombic and cubic structures having the same formula. At $T = 200$ K, the temperature dependences of the resistivity and the permittivity have low-temperature anomalies, which are interpreted as the transition to the orthorhombic phase. The maxima of the permittivity and the resistivity observed at $T = 450$ K are associated with the structural transition to the cubic phase. The nonmonotonic

increase in the permittivity and the minimum in the resistivity observed in the temperature range 200 K < T < 450 K are described in terms of the model of two-phase state with two charge carrier channels.

REFERENCES

1. *Handbook of Sensors and Actuators Series*, Vol. 4: *Semiconductor Sensors in Physico-Chemical Studies* Ed. by L. Yu. Kupriyanov (Elsevier, Amsterdam, 1996).

2. *Chemical Sensors Technology*, Ed. by T. Selyama (Kodansha, Tokyo, 1998), Vol. 1.

3. A. M. Gas'kov and M. N. Rumyantseva, Inorg. Mater. **36** (3), 369 (2000).

4. R. D. Shannon, J. D. Beirlein, and L. J. Gillon, J. Phys. Chem. Solids **41**, 117 (1980).

5. A. Walsh and Graeme W. Watson, Chem. Mater. **19**, 5158 (2007).

6. R. X. Silva, C. W. A. Paschoal, R. M. Almeida, M. Carvalho Castro, Jr., A. P. Ayala, J. T. Auletta, and M. W. Lufaso, Vib. Spectrosc. **64**, 172 (2013).

7. F. Brisse and O. Knop. Can. J. Chem. **46**, 859 (1968).

8. A. Walsh and Graeme W. Watson, Chem. Mater. **19**, 5158 (2007).

9. R. S. Roth, J. Res. Natl. Bur. Stand. (USA) **56**, 17 (1956).

10. E. M. Levin and R. S. Roth, J. Res. Natl. Bur. Stand., Sect. A **68**, 197 (1964).

11. G. Vetter, F. Queyroux, and J. Gilles, Mater. Res. Bull. **13**, 211 (1978).

12. G. Gattow and H. Fricke, Z. Anorg. Allg. Chem. **324**, 287 (1963).

13. N. N. Loshkareva, D. I. Gorbunov, A. V. Andreev, N. V. Mushnikov, Y. Skourski, and F. Wolff-Fabris, J. Alloys Compd. **553**, 199 (2013).

14. M. Respaud, J. M. Broto, H. Rakoto, J. Vanacken, P. Wagner, C. Martin, A. Martin, and B. Raveau, Phys. Rev. B: Condens. Matter **63**, 144426 (2001).

15. A. M. Kadomtseva, Yu. F. Popov, G. P. Vorob'ev, K. I. Kamilov, A. A. Mukhin, V. Yu. Ivanov, and A. M. Balbashov, Phys. Solid State **48** (11), 2134 (2006).

16. M. Respaud, J. M. Broto, H. Rakoto, J. Vanacken, P. Wagner, C. Martin, A. Martin, and B. Raveau, Phys. Rev. B: Condens. Matter **63**, 144426 (2001).

17. N. N. Loshkareva, N. V. Mushnikov, A. V. Koralev, and A. M. Baldashov, Phys. Solid State **51** (4), 773 (2009).

18. A. Maignan, C. Martin, F. Damay, and B. Raveau, Chem. Mater. **10**, 950 (1998).

19. M. P. Kashchenko, *The Wave Model of Martensite Growth for the FCC−BCC Transformation of Iron-Based Alloys* (Nauka, Moscow, 2010) [in Russian].

20. V. Podzorov, B. G. Kim, V. Kiryukhin, M. E. Gershenson, and S.-W. Cheong, Phys. Rev. B: Condens. Matter **64**, 140406(R) (2001).

21. S. Y. Yu., Z. H. Liu, G. D. Liu, J. L. Chen, Z. X. Cao, G. H. Wu, B. Zhang, and X. X. Zhang, Appl. Phys. Lett. **89**, 162503 (2006).

22. V. R. Sharma, M. R. Chattopadhyay, R. Y. B. Shaeb, A. Chauhan, and S. B. Roy, Appl. Phys. Lett. **89**, 222509 (2006).

Translated by Yu. Ryzhkov